3.2.6

Effects of strain rate and temperature on fatigue strength of the mercury target vessel structural material

Xiong Zhihong[1], Takashi Naoe[2], Masatoshi Futakawa[2], Katsuhiro Maekawa[1]
[1]Graduate School of Science and Engineering, Ibaraki University, Hitachi, Ibaraki 316-8511, Japan.
[2]J-PARC Center, JAEA, Tokai, Ibaraki 319-1195, Japan.

E-mail:13nd208n@hcs.ibaraki.ac.jp

Abstract. In the present study, ultrasonic fatigue tests were conducted with controlling specimen surface temperature to investigate the effects of strain rate, temperature and work hardening on very high-cycle fatigue strength of 316L SS. Also, the micro-hardness change due to cyclic fatigue was investigated. The experimental results indicated that the fatigue strengths of solution annealed (SA) and cold worked (CW) at 250 ºC were reduced about 10% and 30% than that of at room temperature, and the fatigue strength was enhanced by the high strain rate. The cyclic hardening occurred in the region of very high-cycle fatigue in the case of SA 316L. In contrast, in the case of 10% CW 316L, cyclic softening occurred when the number of cycles is below 10^6 and followed by cyclic hardening. In the case of 20% CW 316L, the cyclic softening was observed when the number of cycles is below 10^7, while the cyclic hardening occurred subsequently. Furthermore, the sharp increase of the surface temperature was observed in both SA and CW specimens just before the fatigue failure.

1. Introduction

A high-power pulsed spallation neutron source, Japan Spallation Neutron Source (JSNS), is installed at the Materials and Life science experimental Facility (MLF), in the Japan Proton Accelerator Research Complex (J-PARC). High-power pulsed proton beams with an energy of 3 GeV and a power of 1 MW are injected into the liquid mercury to produce spallation neutrons [1]. An enclosure vessel of liquid mercury, a so-called target vessel as shown in figure 1, is made of type 316L austenitic stainless steel (316L SS), which has been widely used in the nuclear industry because of its excellent ductility, corrosion resistance, and irradiation performance. The target vessel is suffered from the cyclic loading due to the proton beam-induced pressure waves [1]. In the case of the JSNS, the repeated proton injection frequency is 25 Hz, and the lifetime is designed to be 2500 hours from the viewpoint of the radiation damage. Therefore, the number of loading cycles will achieve beyond 10^8 cycles, very high-cycles throughout the expected lifetime. The fatigue limit of the 316L SS stainless steel has decreased about 40% by the peak-peak roughness of the pitting damaged surface when the

[1] Graduate School of Science and Engineering, Ibaraki University, Hitachi, Ibaraki 316-8511, Japan.

number of loading cycles gets to be 10^8 [2]. It is reported that the very high-cycle fatigue degradation is different from the conventional fatigue up to million cycles, and the fatigue crack initiation due to internal flaw and/or inclusion becomes dominant in very high-cycle fatigue [3]. The strain rate at the beam window portion of the target vessel is estimated to be 50 1/s at the maximum (as shown in figure 2), which is relatively higher than that of the conventional fatigues. The fatigue strength is affected by the strain rate, i.e., the increase of fatigue lifetime with increasing strain rate [4, 5]. Furthermore, the temperature at the beam window will reach up to 250 ºC due to heat deposit at 1MW operation.

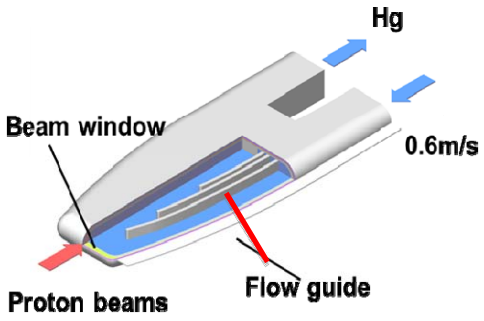

Figure 1. Mercury target vessel at the JSNS

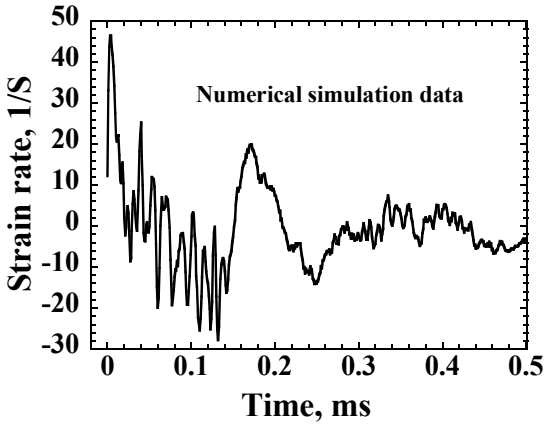

Figure 2. Time response of strain rate at the center part of the beam window

The mercury target vessel is exposed to intense fluxes of protons and spallation neutrons. Irradiation induced defects (frank loops essentially) act as dispersed barriers to dislocation motion, and are responsible for the observed increase in yield stress and the ductility loss. Simultaneously, grain boundaries can be weakened by irradiation, and radiation-embrittlement can lead to crack formation when an irradiated material is subject to cyclic stress loading [6].

Additionally, Liquid Metal Embrittlement (LME) due to mercury immersion is concerned for the mercury target vessels, and is investigated through micro-hardness measurement and bending fatigue testing [7-9]. It was reported that the surface of 316L SS got to be harder and the crack propagation rate was accelerated caused by mercury immersion.

The mechanical properties including high-cycle fatigue behavior and deformation mechanisms of type 316L have been reported in detail [9-11]. There are few researches on the fatigue behavior of type 316L in very high-cycle fatigue region. In the present study, in order to investigate the fatigue strength of the type 316L in high-strain rate, very high-cycle fatigue tests were conducted by using an ultrasonic fatigue-testing machine. Also, the fatigue strength at the temperature of 250 ºC was investigated.

2. Experimental procedure

2.1. Specimen

The type 316L austenitic stainless steel was used for the very high-cycle fatigue test. A part of the as-received materials, which were heat-treated at 1055 ºC for 6 min with water quench (referred to SA), were subjected to different cold-rolled levels, i.e., 10% and 20% reduction of thickness (referred to 10% CW and 20% CW).

An hourglass shape specimen was selected for the test as shown in figure 3. In order to obtain the resonance frequency of the specimen at 20 kHz, the lengths of l and L were selected as 22.7 mm and 40 mm, respectively.

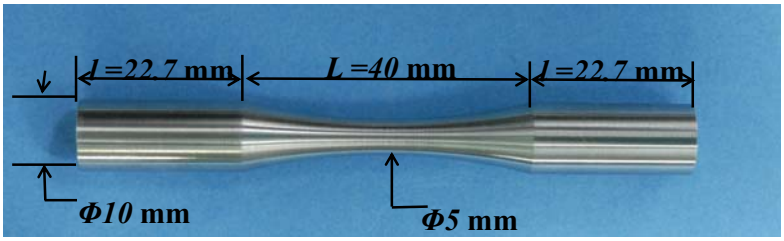

Figure 3. Photograph of the fatigue specimen

2.2. Fatigue test

Load-controlled fatigue tests were conducted by using an ultrasonic fatigue testing system (Shimadzu, USF-2000) as shown in figure 4. The specimen was loaded in tension-compression (the ratio of stress $R = \sigma_{max} / \sigma_{min}$ was -1) with a resonance frequency of 20 kHz. Fatigue failure of the specimen was defined as the resonance frequency exceeded to ±500 Hz of the initial state due to the occurrence of micro-crack. This means that the specimen is not completely broken after the fatigue test. The maximum number of load cycles in this experiment was set to 10^9. More detailed information for the ultrasonic fatigue test is reported elsewhere [12].

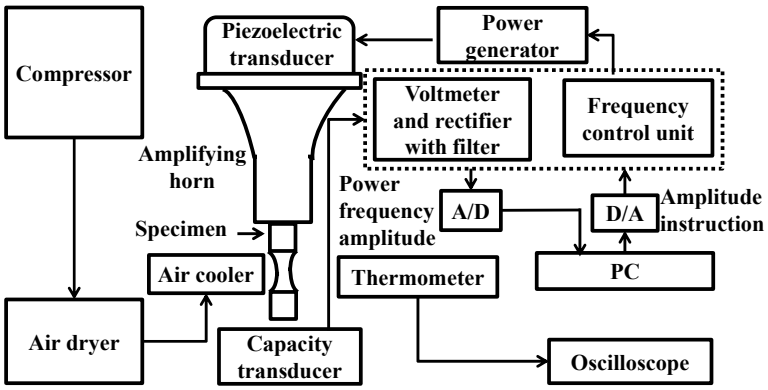

Figure 4. Schematic of ultrasonic fatigue testing machine

In order to prevent an increase of specimen temperature caused by the internal heat generation together with high-speed deformation, loading/arresting intervals were controlled during the test in addition to the air-cooling of the specimen surface. The temperature rise of the center portion of the specimen surface was monitored by using an infrared radiation thermometer (KEYENCE, IT2-02), with a spot diameter of ca. 1.2 mm.

In this research, the self-heating of the specimen during the ultrasonic fatigue test was used for increasing specimen-temperature in order to perform the fatigue test at the temperature of approximately 250 ºC. The fatigue test was carried out as follows: 1) starting the ultrasonic fatigue test without cooling and with the intermittent loading, where the loading time and arresting time were selected according to the stress amplitude; 2) applying the air cooler when the specimen temperature is reach up to about 260 ºC; and 3) adjusting the flow rate of the cold air to maintain the specimen temperature around 250 ºC.

2.3. Micro-hardness measurement

In order to investigate changes in mechanical properties by cyclic loading, the cross-sectional hardness was measured by using a micro hardness tester with a Berkovich tip (Shimadzu, DUH-W201S). The fatigue-failed specimen was cut in a longitudinal direction, and a center part was used for hardness

measurement. The cut specimens were mounted and polished to a mirror surface by using the colloidal silica liquid abrasive with the particle diameter of 0.06 μm. The universal hardness is defined as the quotient of the test load and the surface area of the indentation under an applied test load, which is obtained by [13]

$$H_u = \frac{L_{\max}}{26.43 D^2_{\max}}, \quad (1)$$

where D_{max} is the maximum depth, and L_{max} is the maximum load.

3. Results and discussion

3.1. Specimen temperature during ultrasonic fatigue test

Figure 5 shows the time histories of the surface temperatures of the specimens during the ultrasonic fatigue test under a constant loading time 0.11 s and arresting time 5.0 s. It is observed that the specimen failed at 7.4×10^6 cycles under 260 MPa for SA and 1.05×10^6 cycles under stress amplitude of 380 MPa for 10% CW, respectively. It can be seen that, in the case of SA, the temperatures of specimen was kept at about 13.5 °C at the maximum. On the other hand, the temperature of the 10% CW gradually increased because of the capacity of air cooler was not enough. Figure 6 shows the time histories of the surface temperatures of the specimens during the ultrasonic fatigue test under the loading time 0.11 s and arresting time 0.99 s for SA and the loading time 0.11 s and arresting time 0.22 s for 10% CW, respectively. The specimens failed at 1.22×10^7cycles under the stress amplitude of 180 MPa for SA and 1.29×10^7 cycles under the stress amplitude of 380 MPa for 10% CW, respectively. It can be seen that the temperature at the surface of specimens was kept at about 250 °C.

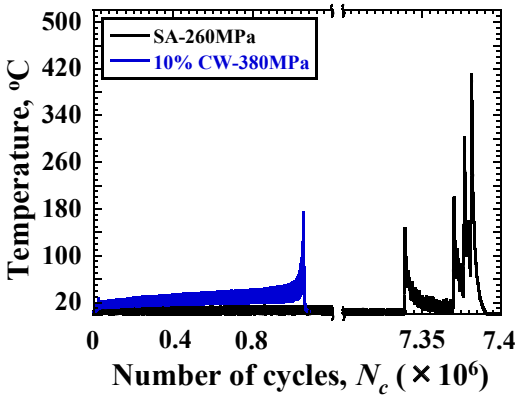

Figure 5. Temperature histories of the specimens tested at room temperature

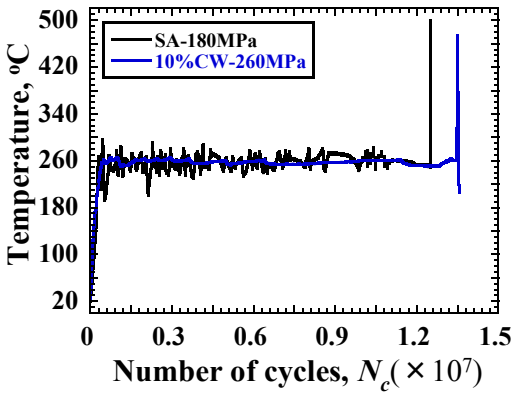

Figure 6. Temperature histories of the specimens tested at 250 °C

At the beginning of the fatigue test around 250 ºC, the temperature rising process (from 0 ºC to 250 ºC) is much less than 1% of the total lifetime. The sharp increases of the surface temperature were noted in both SA and CW specimens just before fatigue failure takes place regardless of the testing temperature. This trend might be utilized to detect the failure just before it. This phenomenon has also been reported in the steels and aluminum alloys [14]. It was suggested that this sudden increase of the temperature allows determining the number of cycles at crack initiation, and more than 90% of the total life that is devoted to crack initiation. In the case of 316L SS, the temperature increase might be enhanced as compared with that of the other metals because of the low thermal conductivity [15].

3.2. Effect of cord work on fatigue strength

The applied stress amplitude as a function of the number of cycles to failure (*S-N*) of SA, 10% CW and 20% CW are shown in figure 7. The fatigue data were fitted according to the Wöhler's approach as follows,

$$\log N_f = a - b\log\sigma_a \tag{2}$$

where σ_a is the stress amplitude, and a and b are constants.

The fatigue failure occurred beyond 10^7 cycles, i.e. in the very high-cycle fatigue regime for the SA, 10% CW and 20% CW. A continuous decline, which is usually observed in the very high-cycle fatigue regime for carbon steels [3, 16], is observed in the 316L regardless of the degree of cold working. That is, the conventional fatigue limit disappears, and the fatigue limit only exists at a given number of cycles. The fatigue strengths of SA, 10% CW and 20% CW at the number of cycles of 10^9 are about 190 MPa, 340 MPa and 390 MPa, respectively. The fatigue strength of 20% CW is higher than that of SA and 10% CW, and the fatigue strength increases with increasing CW level under the stress-controlled fatigue. It was suggested that the dislocation density was increased with the CW level [17]. Increments in dislocation density cause the increase of the tensile strength, which will enhance the fatigue strength. The fatigue degradation rates, defined as the slope of the S-N curve above the fatigue limit, are 1/24, 1/36 and 1/117 for SA, 10% CW and 20% CW, respectively; i.e. the fatigue degradation rate decreases with CW level.

3.3. Effect of strain rate on fatigue strength

In order to investigate the effect of strain rate on the fatigue strength of SA, the fatigue data was compared with the reference data [10, 11, 18]. The experiments of references and the ultrasonic fatigue test were conducted with strain rate magnitude from 10^{-3} to 10^{-1} 1/s and 10^2 1/s, respectively. It can be seen in figure 8 that there are almost no differences in the fatigue lifetime when the frequency is increased from 0.2 Hz to 20Hz (equivalent strain rates from 10^{-3} 1/s to 10^{-1} 1/s). In contrast, the fatigue lifetime exhibits a great increase when the strain rate is increased up to 10^2 1/s. Besides, the effect of strain rate on fatigue limit gets to be more pronounced at high strain rate around 10^2 1/s.

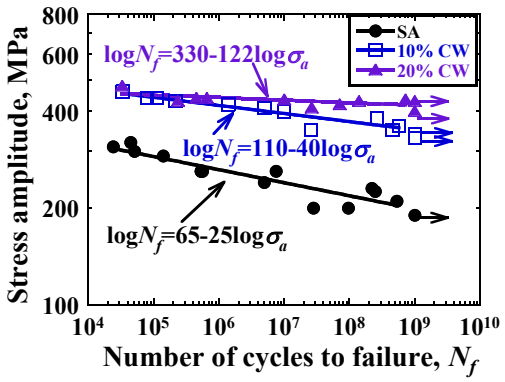

Figure 7. S-N curves of SA, 10% CW and 20%CW

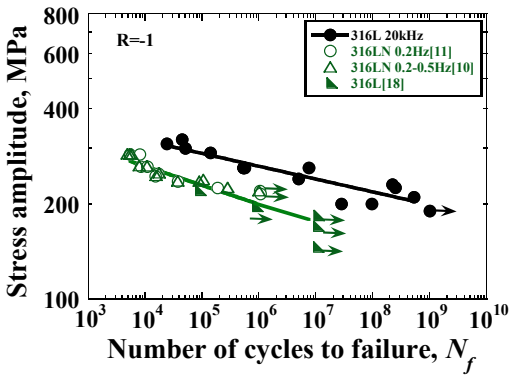

Figure 8. S-N curves of the type 316 SS with different strain rate [10, 11, 18]

Other researchers have reported similar results. In the study on 50CrMo4 [19], the fatigue lifetime increased with the increasing strain rate was also observed. In 316L austenitic stainless steel [20], the decrease of the fatigue lifetime in the low strain rate was considered due to the higher crack density and the decrease in crack propagation rate or cracks initiation life caused by the more pronounced dynamic strain aging at the low strain rate. Moreover, the dynamic strain aging range of the austenitic stainless steel has been proved from 200 °C to 800 °C [21]. Therefore, the increment in fatigue lifetime in the present research should be independent of the dynamic strain aging. Some researchers

suggested that the strength is enhanced at high strain rate [22, 23], which causes the increase of the fatigue strength. Some other researchers [23, 24] considered that the reason of the longer fatigue lifetime at the high strain rate is the slower fatigue crack propagation rate. From this viewpoint, the following model summarized from many experimental data for various materials is used to describe the effect of the testing loading frequency on the fatigue crack propagation rate as follows [24]:

$$\frac{da}{dN} = C_0 f^{-\lambda} (\Delta K)^n \tag{3}$$

where f is the loading frequency, n and C_0 are constants related to the combination of material, temperature and environment, $\triangle K$ is the range of stress intensity factor. From this model, it can be seen that the fatigue crack propagation rate decreases with increasing loading frequency. In the study of 304 austenitic stainless steel [23], the increment in fatigue lifetime is considered due to the deceleration of the fatigue crack propagation and the delay of the crack initiation. Basing on the SEM observation, the striation spacing, which corresponds to the macroscopic crack propagation rate, decreased with increasing strain rate [23].

3.4. Fatigue strength at 250 °C

The applied stress amplitude as a function of the number of cycles to failure (*S-N*) of SA, 10% CW and 20% CW under room temperature (referred to RT) and 250 °C (referred to HT) are shown in figure 9. It can be seen that the fatigue failure occurred beyond 10^7, i.e. in the very high-cycle fatigue regime independent of the testing temperature. The fatigue strengths of SA and 10% CW at 250 ºC were reduced about 10% and 30% than that of at RT, respectively.

It is well known that the fatigue strength of metals and alloys depends on their mechanical properties, such as ultimate tensile strength (UTS). In general, the decreasing in ultimate tensile strength will lead to the decreasing of fatigue strength. Figure 10 shows changes in engineering UTS of SA and 17% CW as a function of temperature [25]. It was indicated that the engineering UTS decreases with increasing temperature. Therefore, the decreasing of fatigue strength at 250 °C is due to the decreasing engineering UTS.

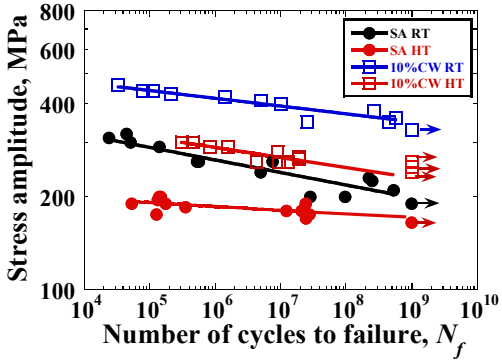

Figure 9. S-N curves of SA and 10% CW under room temperature and 250 °C

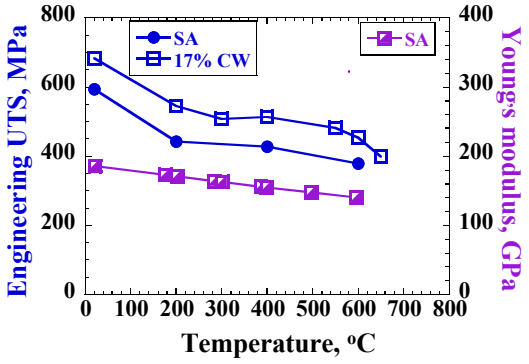

Figure 10. Relationship between engineering UTS, young's modulus and temperature [23, 26]

It has been reported that the reduction of fatigue lifetime at the temperature around 250 °C was attributed to the effect of dynamic strain aging, which occurs in the range from 200 °C to 800 °C in the case of austenitic stainless steel [21, 25, 26]. There are two ways of the dynamic strain aging effect on the fatigue resistance. One is that the dynamic strain aging induces inhomogeneity of deformation lead to the multiple crack initiation, which causes the reduction of the crack initiation life, that is, the fatigue resistance decreases in the crack initiation stage [21]. Another is that dynamic strain aging induced embrittlement can cause a large stress concentration at the crack tip, which will enhance the

crack propagation rate. That is, the fatigue resistance decreases in the crack propagation stage [25]. Kim et al. [27] have also noted that the increasing of crack propagation rate of 316L stainless steel in the dynamic strain-aging regime. In conclusion, the reduced crack initiation life and propagation life caused by the dynamic strain aging lead to the decrease of the fatigue resistance in the regime of dynamic strain aging. Srinivasan et al. [26] have suggested that the effect of the oxidation of the specimen will enhance the crack nucleation at slip steps. The fatigue resistant of 316L in the air was proved to be weaker than that of in the vacuum [28]. However, in the present research, the oxidation of the specimen during the fatigue tests at around 250 °C is hardly observed. Hence, the effect of the oxidation of the specimen on fatigue strength can be negligible.

During the fatigue test at 250 °C, the frequency decreases with increasing temperature until it reach up to 250 °C, as shown in figure 11. The reduction of resonance frequency induced by the temperature of 250 °C is about 400Hz, which is very small compared with that of 20 kHz at room temperature. Therefore, the effect of the resonance frequency caused by the testing temperature should not be considered. The decreasing in resonance frequency can be attributed to the decreasing in Young's modulus, which has been reported that the Young's modulus decreases with increasing temperature [28], as shown in figure 10.

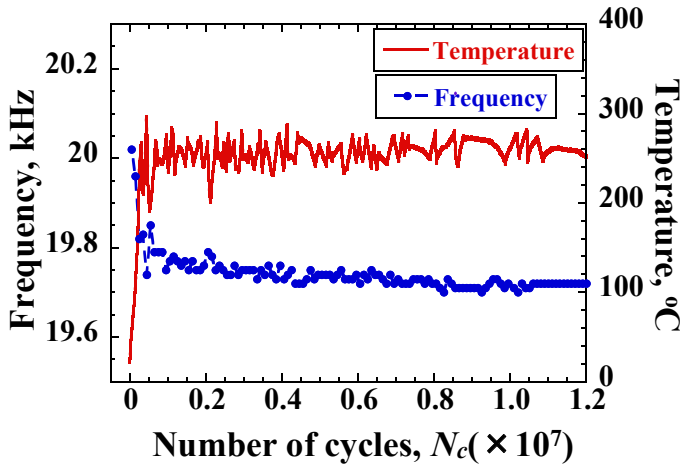

Figure 11. Frequency and specimen temperature of SA during fatigue test at 180MPa

3.5. Micro-hardness change during fatigue test

Changes in universal hardness of fatigue-failed specimens with the different number of cycles are indicated in figure 12. In the case of SA, the universal hardness shows an increase with the number of cycles: that is, a so-called cyclic hardening is recognized. In contrast, the hardness and residual strength of 10% CW show the negative relation with the number of cycles in the region below 10^6: a so-called cyclic softening is recognized, and thereafter the cyclic hardening occurs. Furthermore, in the case of 20% CW, there exists the negative relationship between the universal hardness and the number of cycles when the number of cycles is below about 10^7, i.e. cyclic softening occurs, followed by cyclic hardening. A similar tendency of the universal hardness can be seen in 10% CW, but the break point, i.e. the number of cycles when the cyclic hardening transit from cyclic softening, seems to shift to 10^7 cycles approximately.

The cyclic hardening for annealed materials [29, 30] and cyclic softening for the pre-strained materials [20, 21] in the low cycle strain-controlled fatigue have been observed. It was supposed that the cyclic behavior, i.e. cyclic hardening or softening, is related to the interaction between the plastic deformation induced by dislocation generation rate and annihilation rate [31, 32]. When the

annihilation rate of dislocation is lower than the generation rate, the dislocation density will increase, and the cyclic hardening takes place. Otherwise, cyclic softening occurs.

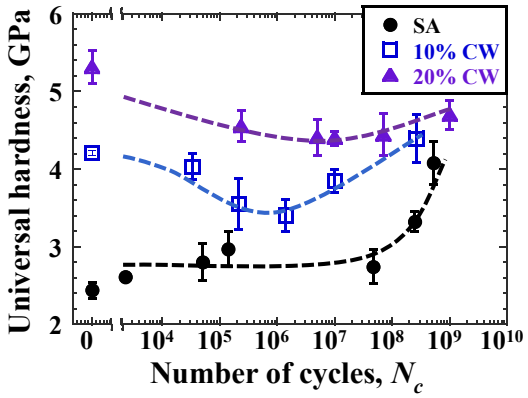

Figure 12. Relationship between hardness and the number of cycles

4. Summary

The followings are summarized from the ultrasonic fatigue tests on 316L SS:

1) The fatigue failure occurred beyond 10^7 cycles, i.e. in the very high-cycle regime, independent of the testing temperature.

2) The fatigue strength increases with the cold work level.

3) The fatigue limit at a high strain rate (10^2 1/s) is higher than that of the lower strain rate (10^{-3} 1/s to 10^{-1} 1/s).

4) The fatigue strengths of SA and 10% CW of 250 ºC were reduced about 10% and 30% from that of room temperature, respectively.

5) The cyclic behavior of the materials is dependent on their initial state, pre-strained or not. In the case of solution annealed (SA) 316L, the universal hardness showed a positive relation with the number of cycles: i.e. cyclic hardening occurred. On the contrary, in the case of cold worked (CW) 316L, the universal hardness showed a negative relation with the number of cycles, followed by cyclic softening when the number of cycles smaller than a critical value. The critical number of cycles is about 10^6 for 10% CW and 10^7 for 20% CW.

6) A sharp increase of the surface temperature was observed in both SA and CW specimens just before fatigue failure regardless of the testing temperature. This phenomenon can be applied to detect fatigue failure.

5. Acknowledgments

This research was partly supported by Japan Society for the Promotion of Science through a Grant-in-Aid for Scientific Research (No. 23360088 and 26820016).

References

[1] Futakawa M, Haga K, Wakui T, Kogawa H and Naoe T 2009 *Nucl. Instr. Meth. Phys. Res. A*. **600** 18-21
[2] Futakawa M, Wakui T, Kogawa H and Ikeda Y 2006 *Nucl. Instr. Meth. Phys. Res. A*. **562** 676-79
[3] Li X 2012 *J. Int. Mater. Rev.* **57** 92-110
[4] Wu J, Lin C 2005 *J. Mater. Sci. Eng. A*. **390** 291-98
[5] Hong S, Lee S 2005 *J. Nucl. Mater.* **340** 307-14
[6] Mansur L 2006 *Nucl. Instr. Meth. Phys. Res. A*. **562** 666-75
[7] Naoe T, Yamaguchi Y, Futakawa M 2012 *J. Nucl. Mater.* **431** 133-39

[8] Futakawa M, Wakui T, Kogawa H, Date H 2002 *Int. Conf. on Materials and processing* **Vol 1** (Honolulu: Hawaii) pp538-563
[9] Strizak J P, Mansur L K 2003 *J. Nucl. Mater.* **318** 151-56.
[10] Strizak J P, Tian H, Liaw P k, Mansur L K 2005 *J. Nucl. Mater.* **343** 134-44.
[11] Tian H, Liaw P k, Strizak J, Mansur L 2003 *J. Nucl. Mater.* **318** 157-66.
[12] Xiong Z H, Futakawa M, Naoe T, Maekawa K 2014 Adv. Mater. Res. **891-892** 536-541.
[13] Weiler W 1992 Atalanta *The proceedings of the 79th AESF annual technical conference* AESF Inc. pp 277-284
[14] Wagner D, Ranc N, Bathias C, Paris P C 2009 *Fatigue Fract. Engng. Mater. Struct.* **33** 12-21
[15] Akai A, Shiozawa D, Sakagami T 2013 *J. Soc. Mate. Sci.* **62** 554-64 (In Japanese)
[16] Sakai T, 2009 *J. Solid Mech. Mater. Eng.* **3** 425-39
[17] Ohtani T, Ogi H, Hirao M 2005 *Metall. Mater. Trans A.* **36** 411-20
[18] Huang J Y, Yeh J J, Jeng S L, Chen C Y, Kuo R C 2006 *Materials Transactions* 47 409-17
[19] Schneider N, Pyttel B, Berger C and Oechsner M, 2014, *Adv. Mater. Res.* **891-892** 1430-35
[20] Hong S G, Lee K O, and Lee S B, 2005, *Int.J. Fatigue* **27** 1420-24
[21] Hong S G, Lee S B, 2005, *J. Nucl. Mater.* **340** 307-14
[22] Schneider N, Pyttel B, Berger C, Oechsner M, 2014 Adv. Mater. Res. **891-892** 1430-35
[23] Kawata K, Miyamoto I, Itabashi M 1987 proceeding of IMPACT`87 **Vol 1** (Bremen, Germany) pp349-56
[24] Poulain T, Mendez J, Henaff G, Baglion L D, *2014 Adv. Mater. Res.* **891-892** 1420-26
[25] Shih Y S, Chen J J, 1999 *Nucl. Eng. Design* **191** 225-30
[26] Hong S G, Yoon S, and Lee S B, 2003, *Int.J. Fatigue* **25** 1293-300
[27] Srinivasan V S, Sandhya R, Bhanu Sankara Rao K, Mannan S L, Raghavan K S 1991 *Int.J. Fatigue*, 13(1991) 471-78.
[28] Kim D W, Kim W G, Ryu W S, 2003 *Int.J. Fatigue* **25** 1203-07
[29] Alain R, Violan P, Mendez J, 1997 Mater. Sci. Eng. A **229** 87-94
[30] Yu D, An K, Chen Y, Chen X, 2014, *Scripta Mater.* **89** 45-48
[31] Mughrabi H, 1978 *Mater. Sci. Eng.* **33** 207-23
[32] Stephens R I, Fatemi A, R. Stephens R, Fuchs H O 2001 *Metal Fatigue in Engineering* (New York: John Wiley & Sons) p 44
[33] Galindo-Nava E I, Sietsma J, Rivera-Díaz-del-Castillo P E J 2012, *Acta. Materialia*. **60** 2615-24.